

Measurement of $W\gamma$ and $Z\gamma$ production in proton-proton collisions at $\sqrt{s} = 7$ TeV with the ATLAS Detector

Song-Ming Wang^{*†}

Institute of Physics, Academia Sinica, Taiwan

E-mail: smwang@phys.sinica.edu.tw

We present studies of W and Z bosons with associated high energy photons produced in pp collisions at $\sqrt{s} = 7$ TeV. The analysis uses 35 pb^{-1} of data collected by the ATLAS experiment in 2010. The event selection requires W and Z bosons decaying into high p_T leptons (electrons or muons) and a photon with $E_T > 15$ GeV separated from the lepton(s) by a distance $\Delta R(l, \gamma) > 0.7$ in η - ϕ space. A total of 95 (97) $pp \rightarrow e^\pm \nu \gamma + X$ ($pp \rightarrow \mu^\pm \nu \gamma + X$) and 25 (23) $pp \rightarrow e^+ e^- \gamma + X$ ($pp \rightarrow \mu^+ \mu^- \gamma + X$) event candidates are selected. The kinematic distributions of the leptons and photons and the production cross sections are measured. The data are found to agree with Standard Model predictions that include next-to-leading-order $O(\alpha\alpha_s)$ contributions.

*The 2011 Europhysics Conference on High Energy Physics-HEP 2011,
July 21-27, 2011
Grenoble, Rhône-Alpes France*

^{*}Speaker.

[†]for the ATLAS Collaboration



1. Introduction

Measurements of W and Z bosons productions in association with high energy photons provide important tests of the Standard Model (SM) of particle physics. The $W\gamma$ process is directly sensitive to the triple gauge boson couplings predicted by the non-Abelian $SU(2)_L \times U(1)_Y$ gauge group of the electroweak sector. However, the triple gauge boson couplings in the $Z\gamma$ process is forbidden in the SM at tree level. Physics beyond the SM can enhance the production cross sections and alter the event kinematics.

The $W\gamma$ and $Z\gamma$ productions are studied through the measurement of $pp \rightarrow l^\pm \nu \gamma + X$ and $pp \rightarrow l^+ l^- \gamma + X$ production at $\sqrt{s} = 7$ TeV with the ATLAS detector [1], with an integrated luminosity of approximately 35 pb^{-1} [2]. The studies are performed in the electron and muon decay channels, The sources of the $l^\pm \nu \gamma$ and $l^+ l^- \gamma$ final states are $W\gamma \rightarrow l^\pm \nu \gamma$ and $Z\gamma \rightarrow l^+ l^- \gamma$ production, as well as QED final state radiation (FSR) from inclusive W and Z production: $W \rightarrow l^\pm \nu \rightarrow l^\pm \nu \gamma$, $Z \rightarrow l^+ l^- \rightarrow l^+ l^- \gamma$ (figure 1). The final state also include events with photons coming from hard fragmentation of a quark or gluon (see figure 1(d) for the case of $l\nu\gamma$ with photon from quark fragmentation).

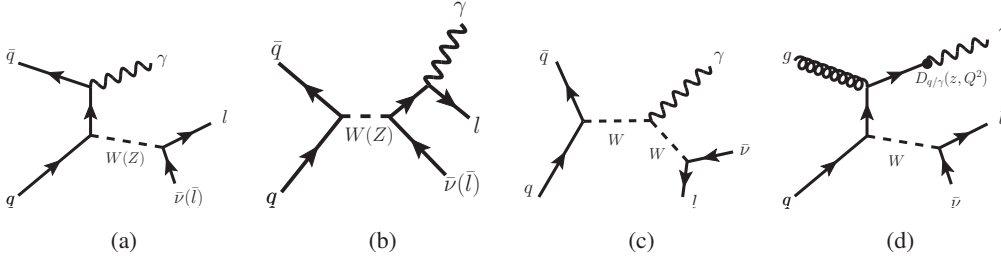


Figure 1: Feynman diagrams of $W\gamma$ and $Z\gamma$ production with (a) photon from initial state radiation and (b) final state photon radiation from the W and Z boson decay process. (c) Feynman diagram of $W\gamma$ production in the s-channel. (d) Diagram of the signal contribution from the $W + q$ process when a photon emerges from the fragmentation of the final state quark.

2. Selection of $W\gamma$ and $Z\gamma$ candidates

A $W\gamma$ candidate event is required to have an isolated electron or muon with transverse momentum $p_T(l) > 20$ GeV, an isolated photon with transverse energy $E_T(\gamma) > 15$ GeV, missing transverse energy $E_T^{\text{miss}} > 25$ GeV and the transverse mass of the lepton- E_T^{miss} system $m_T(l, \nu) > 40$ GeV, where $m_T(l, \nu) = \sqrt{2p_T(l) \cdot E_T^{\text{miss}} \cdot (1 - \cos \Delta\phi)}$, and $\Delta\phi$ is the azimuthal separation between the directions of the lepton and the missing transverse energy vector. The photon is required to be separated from the nearest lepton by $\Delta R(l, \gamma) > 0.7$ to reduce the FSR contribution, and its isolation transverse energy E_T^{iso} recorded in the calorimeter around the photon in a cone size of $\Delta R = 0.4$ (excluding the photon cluster) to be less than 5 GeV. The leptons and photon are required to be identified in the pseudorapidity range ($|\eta| < \sim 2.4$) where the detector has good acceptance. In the $Z\gamma$ analysis, each signal candidate event is required to have an isolated photon in the final state and the invariant mass of the two opposite charged leptons is required to be greater than 40 GeV. All the requirements on the leptons and photon are the same as in the $W\gamma$ analysis except a looser

electron identification criteria is applied in the $Z\gamma$ analysis. The efficiencies to identify an electron, a muon and a photon are $\sim 70 - 90\%$ (tight or loose selection criteria), $\sim 88\%$ and $\sim 70\%$, respectively. The numbers of selected $W\gamma$ and $Z\gamma$ events are presented in Table 1. The distributions of the transverse energy of the photon from the $W\gamma$ candidate events and the three body invariant mass $m_{l+l-\gamma}$ from the $Z\gamma$ candidate events are shown in figure 2.

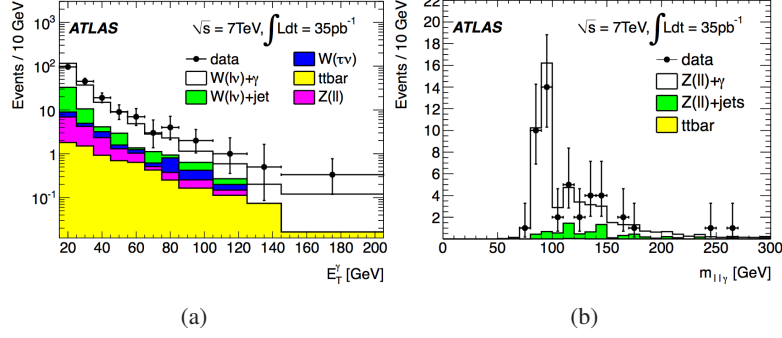


Figure 2: Distributions for the combined electron and muon decay channels of the (a) photon transverse energy of the $W\gamma$ candidate events and (b) three body invariant mass $m_{l+l-\gamma}$ distribution for $Z\gamma$ candidate events.

3. Background Determination and Signal Yield

The dominant sources of background for this analysis are from $W(Z)$ +jets productions where the jets are mis-identified as photons. As the jet faking photon rate is not well modeled by Monte Carlo (MC) simulation, the W +jets background is estimated from the ATLAS data for the $W\gamma$ analysis. For the $Z\gamma$ analysis, due to limited statistics, the Z +jets background is estimated with MC and is assigned a large uncertainty. Additional backgrounds from other processes, such as $W \rightarrow \tau\nu$, $t\bar{t}$, and $Z \rightarrow e^+e^- (\mu^+\mu^-)$ (misidentified as $W\gamma$) for the $W\gamma$ analysis, and $t\bar{t}$ and Z +jets for the $Z\gamma$ analysis will be referred to collectively as “EW+ $t\bar{t}$ background” and their contribution is estimated from MC simulation. The W +jets background in the $W\gamma$ analysis is estimated with a two-dimensional side band method that makes use of the E_T^{iso} variable and the identification “quality” variable of the photon to define three control regions that are used for estimating the W +jets contribution in the signal region. This method assumes that these two variables are not highly correlated for the W +jets background. The number of observed candidate events and the estimated number of background and signal events are shown in Table 1.

Process	Observed	EW+ $t\bar{t}$	W +jets	Signal
$N_{obs}(W\gamma \rightarrow e^\pm \nu\gamma)$	95	$10.3 \pm 0.9 \pm 0.7$	$16.9 \pm 5.3 \pm 7.3$	$67.8 \pm 9.2 \pm 7.3$
$N_{obs}(W\gamma \rightarrow \mu^\pm \nu\gamma)$	97	$11.9 \pm 0.8 \pm 0.8$	$16.9 \pm 5.3 \pm 7.4$	$68.2 \pm 9.3 \pm 7.4$
Process	Observed	EW+ $t\bar{t}$		Signal
$N_{obs}(Z\gamma \rightarrow e^+e^-\gamma)$	25	3.7 ± 3.7		$21.3 \pm 5.8 \pm 3.7$
$N_{obs}(Z\gamma \rightarrow \mu^+\mu^-\gamma)$	23	3.3 ± 3.3		$19.7 \pm 4.8 \pm 3.3$

Table 1: Numbers of the total observed candidate events and the estimated number of background and signal events for the $W\gamma$ and $Z\gamma$ analyses. Where two uncertainties are quoted the first is statistical and the second is systematic. For the $Z\gamma$ analysis the uncertainty on the MC based background estimate is 100%.

4. Cross Section Measurements

The measurements of the fiducial cross sections for the processes $pp \rightarrow l^\pm \nu \gamma + X$ and $pp \rightarrow l^+ l^- \gamma + X$ in the kinematic phase space defined by the selection cuts, can be expressed as $\sigma_{pp \rightarrow l^\pm \nu \gamma(l^+ l^- \gamma)}^{\text{fid}} = N_{W\gamma(Z\gamma)}^{\text{sig}} / (C_{W\gamma(Z\gamma)} \cdot L_{W\gamma(Z\gamma)})$ where $N_{W\gamma(Z\gamma)}^{\text{sig}}$ denotes the estimated number of $W\gamma(Z\gamma)$ signal events and $L_{W\gamma(Z\gamma)}$ denotes the integrated luminosity for the analysis. $C_{W\gamma(Z\gamma)}$, which is the probability for the events generated within the fiducial region of phase space to pass the final selection requirements, consists of correction factors from the event trigger efficiencies and the selection and reconstruction efficiencies of the photon and leptons. The measured fiducial cross sections are then extrapolated to the production cross section using the equation $\sigma_{pp \rightarrow l^\pm \nu \gamma(pp \rightarrow l^+ l^- \gamma)}^{\text{fid}} = \sigma_{pp \rightarrow l^\pm \nu \gamma(pp \rightarrow l^+ l^- \gamma)}^{\text{fid}} / A_{W\gamma(Z\gamma)}$ where $A_{W\gamma(Z\gamma)}$ is the acceptance of the fiducial phase space with respect to the production phase space. The production phase space is defined by requiring $E_T(\gamma) > 15$ GeV, $\Delta R(l, \gamma) > 0.7$, and the relative isolation $\epsilon_h < 0.5$. ϵ_h is the ratio of the sum of energies carried by the particles emerging from the quark/gluon fragmentation process (excluding the photon) within a cone size of 0.4 surrounding the fragmented photon to the energy carried by the photon. For the $Z\gamma$ case, the invariant mass of the two leading opposite charged leptons to be greater than 40 GeV. The uncertainties on the acceptance correction factors are mainly due to the uncertainties from the reconstruction and identification efficiencies of the photon ($\sim 10\%$) and the electron ($\sim 4.5\%$), and the uncertainties from the electromagnetic energy scale and resolution ($\sim 3 - 4.5\%$). The measured cross sections for $W\gamma$ and $Z\gamma$ productions are presented in Table 2. The measurements are in agreement with the SM predictions.

	Experimental measurement	SM prediction
	$\sigma^{\text{fid}}[\text{pb}]$	$\sigma^{\text{fid}}[\text{pb}]$
$pp \rightarrow e^\pm \nu \gamma$	$5.4 \pm 0.7 \pm 0.9 \pm 0.2$	4.7 ± 0.3
$pp \rightarrow \mu^\pm \nu \gamma$	$4.4 \pm 0.6 \pm 0.7 \pm 0.2$	4.9 ± 0.3
$pp \rightarrow e^+ e^- \gamma$	$2.2 \pm 0.6 \pm 0.5 \pm 0.1$	1.5 ± 0.1
$pp \rightarrow \mu^+ \mu^- \gamma$	$1.4 \pm 0.3 \pm 0.3 \pm 0.1$	1.7 ± 0.1
	$\sigma[\text{pb}]$	$\sigma[\text{pb}]$
$pp \rightarrow e^\pm \nu \gamma$	$41.1 \pm 5.7 \pm 7.1 \pm 1.4$	36.0 ± 2.3
$pp \rightarrow \mu^\pm \nu \gamma$	$33.0 \pm 4.6 \pm 5.5 \pm 1.1$	36.0 ± 2.3
$pp \rightarrow l^\pm \nu \gamma$	$36.0 \pm 3.6 \pm 6.2 \pm 1.2$	36.0 ± 2.3
$pp \rightarrow e^+ e^- \gamma$	$9.9 \pm 2.7 \pm 2.3 \pm 0.3$	6.9 ± 0.5
$pp \rightarrow \mu^+ \mu^- \gamma$	$5.6 \pm 1.4 \pm 1.2 \pm 0.2$	6.9 ± 0.5
$pp \rightarrow l^+ l^- \gamma$	$6.5 \pm 1.2 \pm 1.7 \pm 0.2$	6.9 ± 0.5

Table 2: Fiducial and production cross sections of the $pp \rightarrow l^\pm \nu \gamma + X$ and $pp \rightarrow ll\gamma + X$ process at $\sqrt{s} = 7$ TeV. For the measurements, the first uncertainty is statistical, the second is systematic and the third is from the luminosity. The uncertainty in the SM prediction is systematic.

References

- [1] ATLAS Collaboration, *The ATLAS Experiment at the CERN Large Hadron Collider*, *JINST* **3** (2008) S08003.
- [2] ATLAS Collaboration, G. Aad et al., *Measurement of $W\gamma$ and $Z\gamma$ production in proton-proton collisions at $\sqrt{s} = 7$ TeV with the ATLAS Detector*, *JHEP* **09** (2011) 072.